Supplementary Information

Metallic FeSe Monolayer as Anode Materials for Li and Non-Li Ion Batteries: A DFT Study

Xiaodong Lv,[1] Fengyu Li,[1,*] Jian Gong,[1,*] Jinxing Gu,[2] Shiru Lin,[2] Zhongfang Chen[2,*]

[1] *Physical School of Science and Technology, Inner Mongolia University, Hohhot, China, 010021*

[2] *Department of Chemistry, The Institute for Functional Nanomaterials, University of Puerto Rico, Rio Piedras Campus, San Juan, PR 00931, USA*

*corresponding author: fengyuli@imu.edu.cn (FL); ndgong@imu.edu.cn (JG); zhongfangchen@gmail.com (ZC)

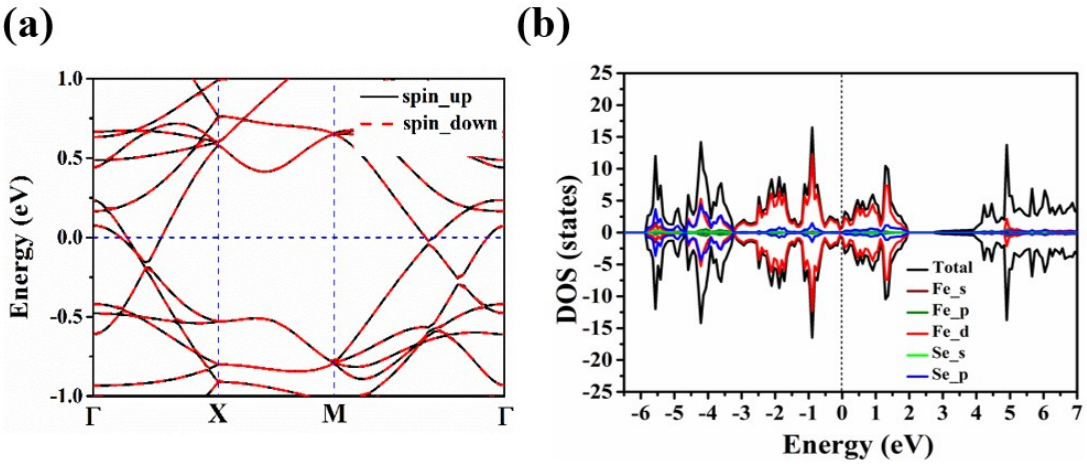

Fig. S1 The PBE+U band structure (a) and density of state (b) for the FeSe monolayer.

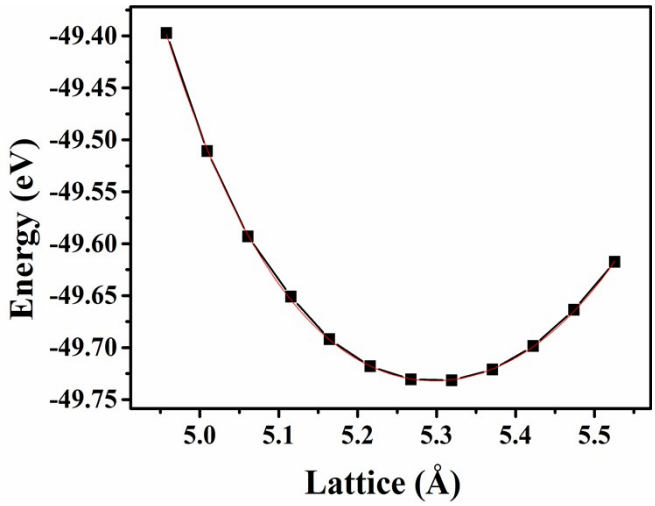

Fig. S2 The total energy of FeSe monolayer AFM states as a function of lattice constant.

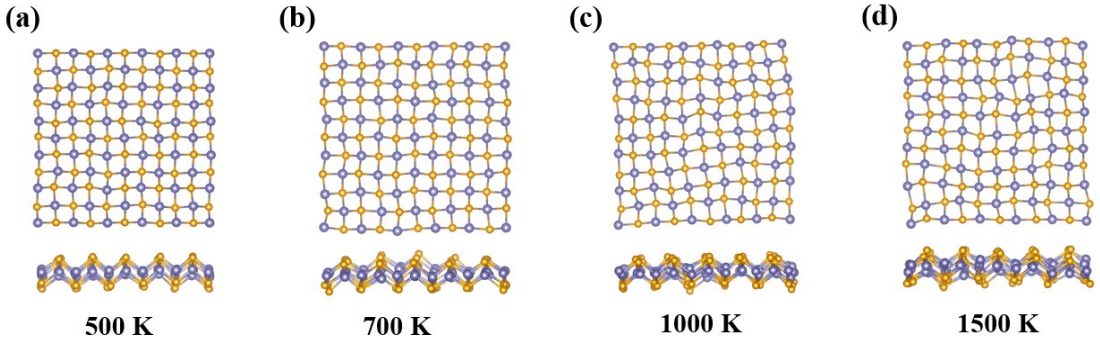

Fig. S3 Top and side views of FeSe monolayers (a 5×5×1 supercll) at the end of the 5 ps MD simulations at the temperature of (a) 500 K (b) 700 K (c) 1000 K and (d) 1500 K, respectively.

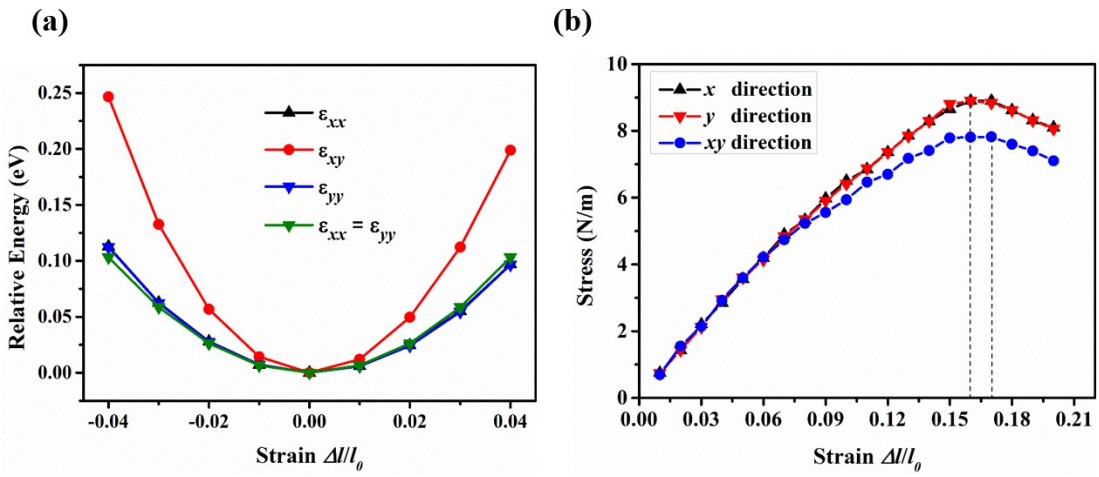

Fig. S4 (a) The relative strain energy of monolayer FeSe under uniaxial, shear and biaxial in-plane strain (-4%≤ε≤4%). (b) The strain-stress relation of FeSe monolayer with applying the uniaxial (*x* and *y* direction) and biaxial (*xy* direction) in-plane strain, respectively.

In Fig. S4a, the strain energies as a function of ε in the range of -4%≤ε≤4% with an increment of 1% were computed to obtain the elastic constants, in order to calculate the Young's modulus [E. Cadelano, P. L. Palla, S. Giordano, L. Colombo, *Phys. Rev. B* 2010, **2**, 235414.].

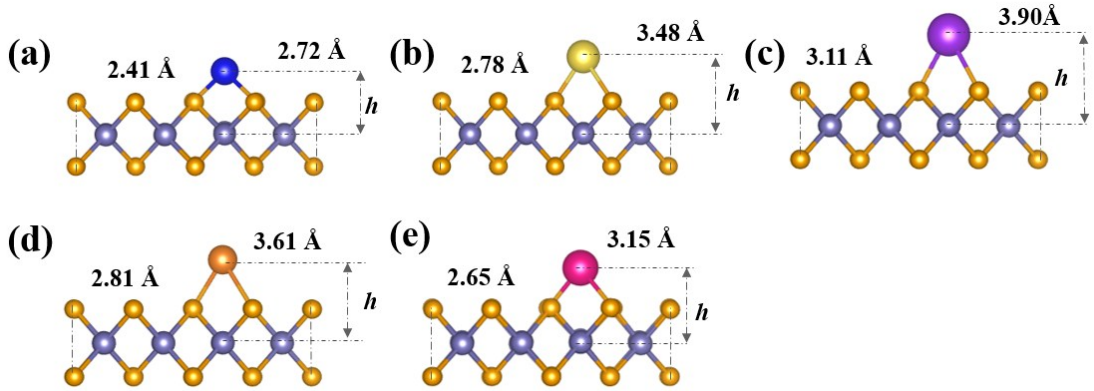

Fig. S5 Sides views of the optimized structures of FeSe monolayer after adsorption with (a) Li, (b) Na, (c) K, (d) Mg and (e) Ca at **B** site.

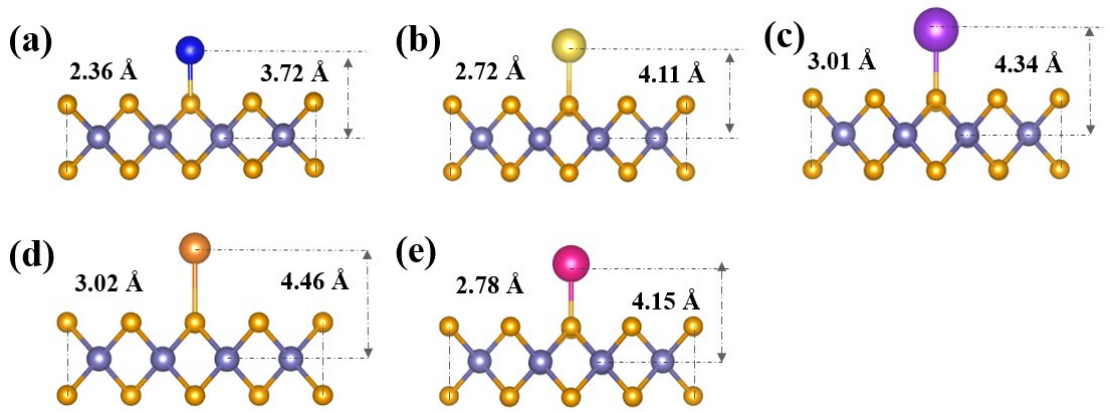

Fig. S6 Sides views of the optimized structures of FeSe monolayer after adsorption with (a) Li, (b) Na, (c) K, (d) Mg and (e) Ca at **C** site.

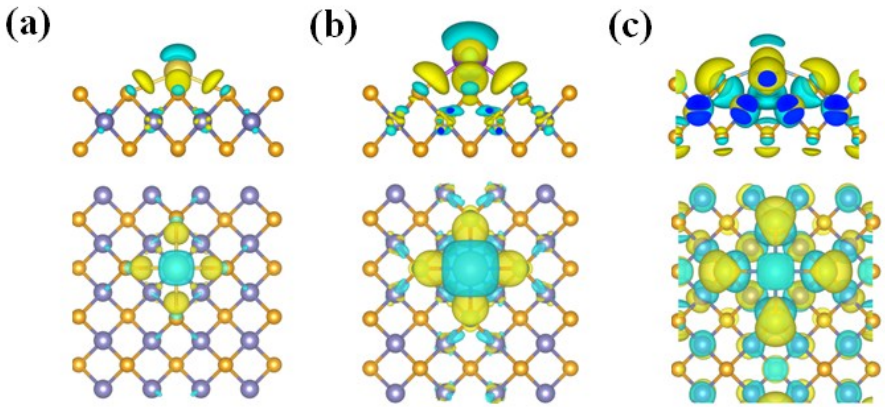

Fig. S7 Charge density differences for M atoms adsorbed FeSe monolayer at **A** site, (a) *M* = Na, (b) *M* = K, (c) *M* = Ca. The isosurface value is set to be 0.002 eÅ^{-3}.

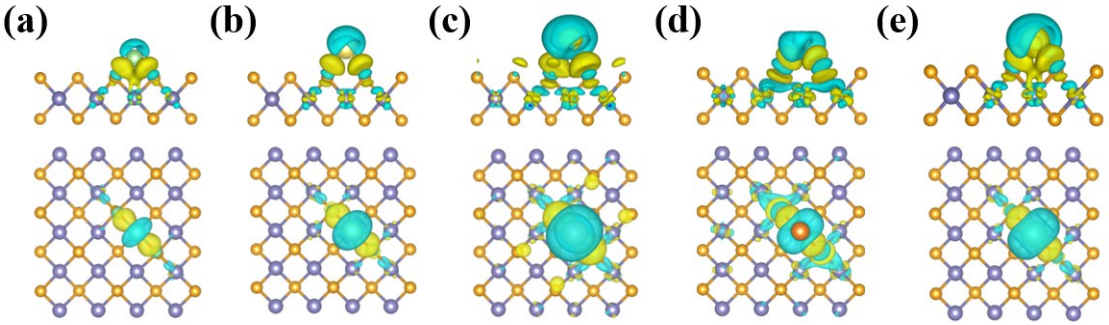

Fig. S8 Charge density differences for M atoms adsorbed FeSe monolayer at **B** site, (a) *M* = Li, (b) *M* = Na, (c) *M* = K, (d) *M* = Mg, and (e) *M* = Ca. The isosurface value is set to be 0.002 eÅ^{-3}.

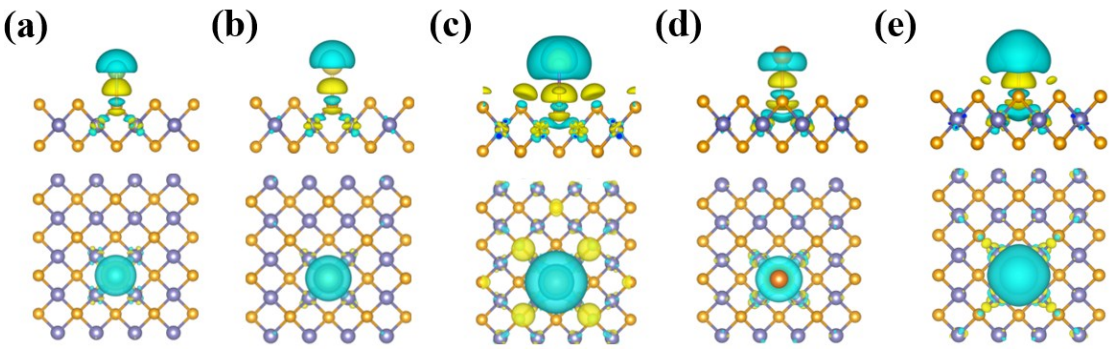

Fig. S9 Charge density differences for *M* atoms adsorbed FeSe monolayer at **C** site, (a) *M* = Li, (b) *M* = Na, (c) *M* = K, (d) *M* = Mg, and (e) *M* = Ca. The isosurface value is set to be 0.002 eÅ^{-3}.

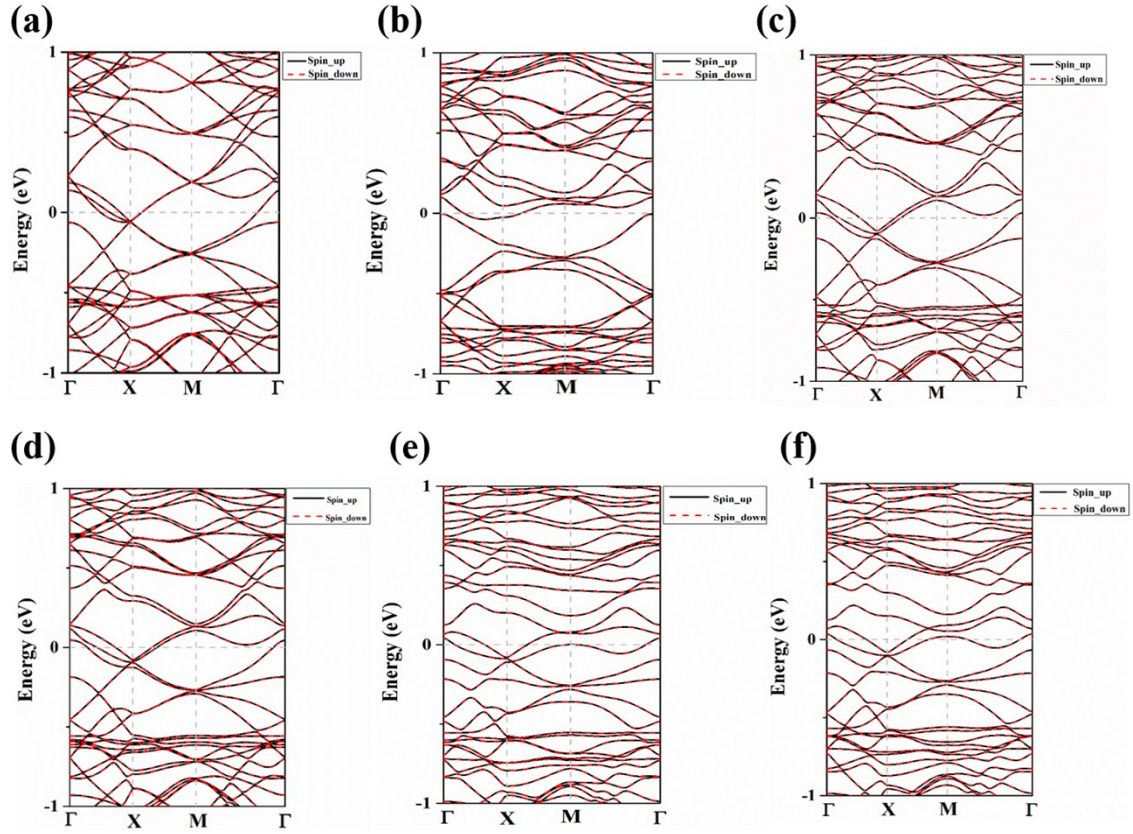

Fig. S10 The band structures of metal atoms adsorbed FeSe monolayers, (a) pristine FeSe monolayer, (b) Li, (c) Na, (d) K, (e) Mg and (f) Ca at **A** site.

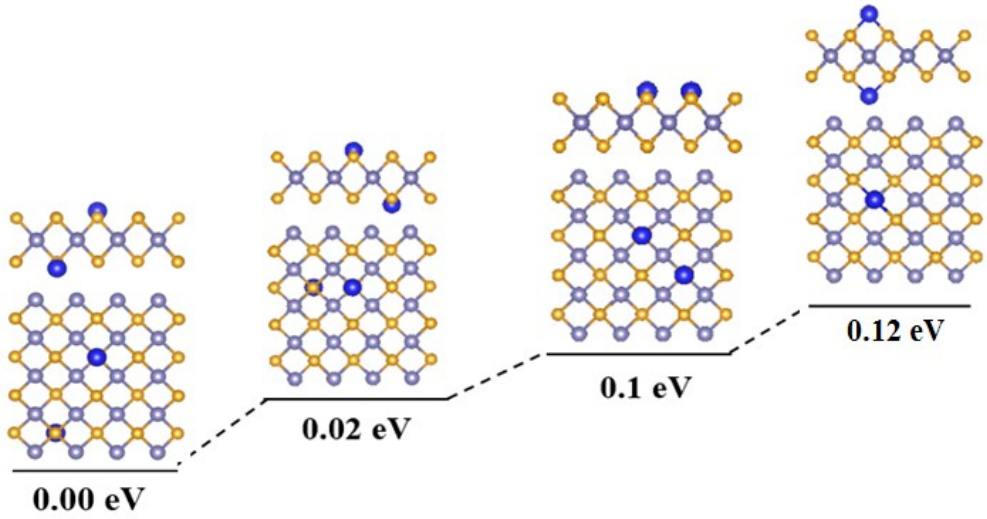

Fig. S11 Side and top views of different configurations for $Li_{0.125}FeSe$ as well as the relative energies.

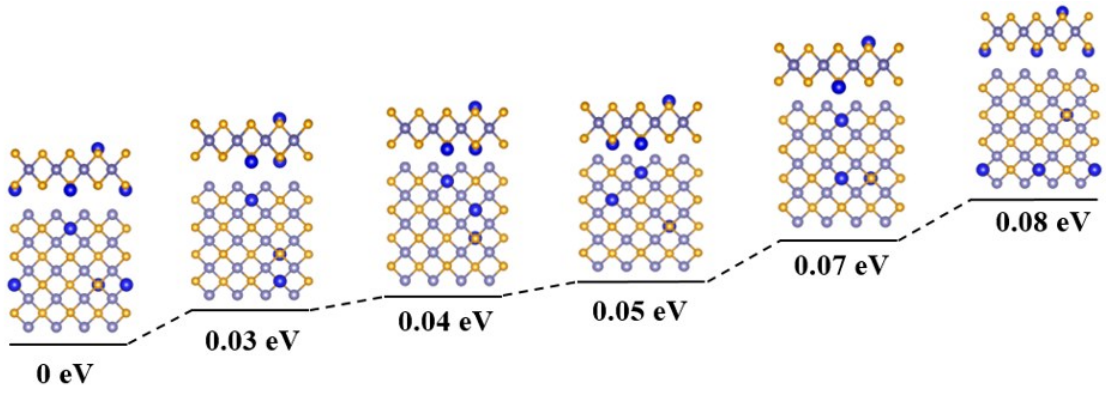

Fig. S12 Side and top views of different configurations for $Li_{0.187}FeSe$ as well as the relative energies.

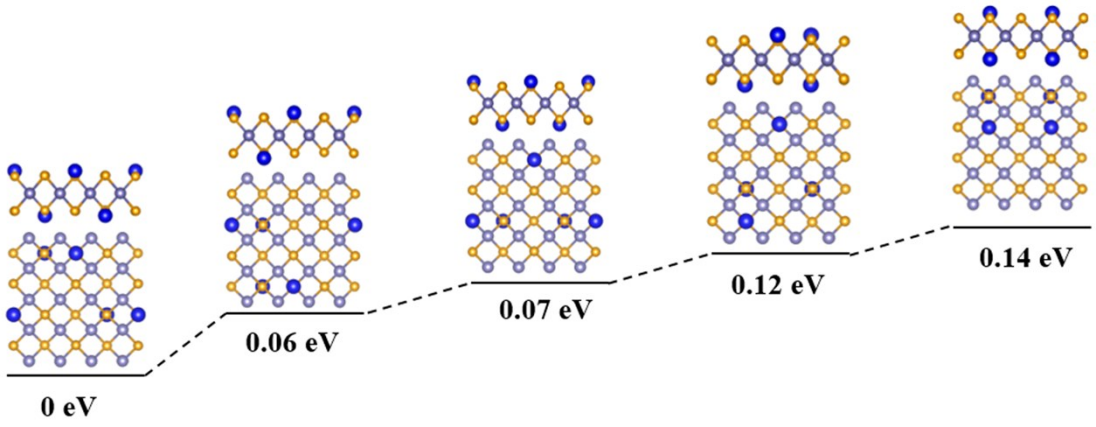

Fig. S13 Side and top views of different configurations for $Li_{0.25}FeSe$ as well as the relative energies.

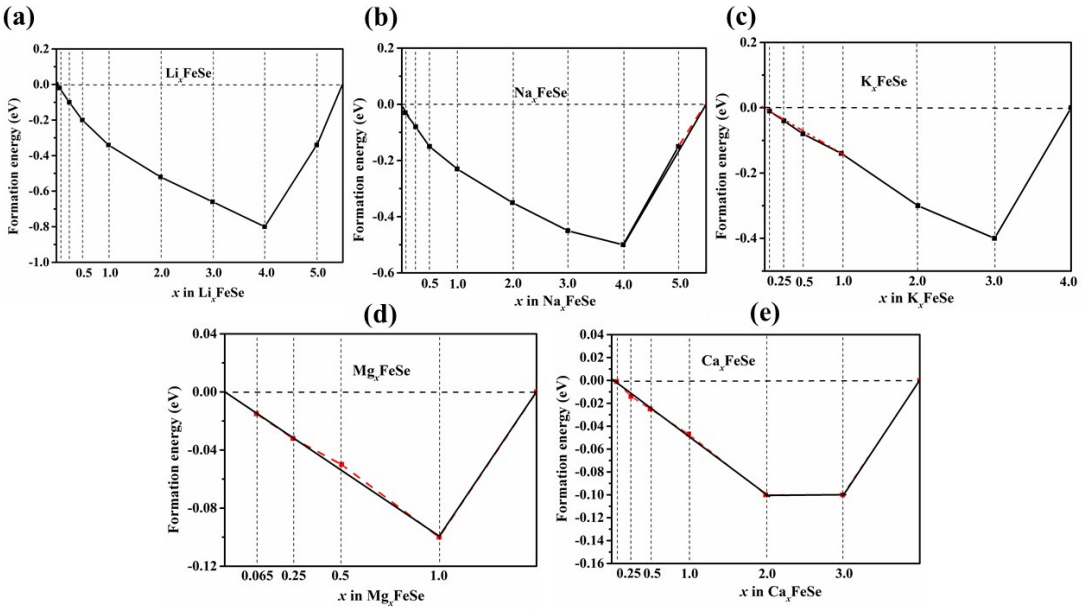

Fig. S14 The formation energies (E_f) of Li_xFeSe (a), Na_xFeSe (b), K_xFeSe (c), Mg_xFeSe (d) and Ca_xFeSe (e) with respect to FeSe sheet and Li/Na/K/Mg/Ca bulk metal. Data points located on the convex hull (black squares) represents the stable adsorption without decomposition. The metastable phases are indicated by red squares.

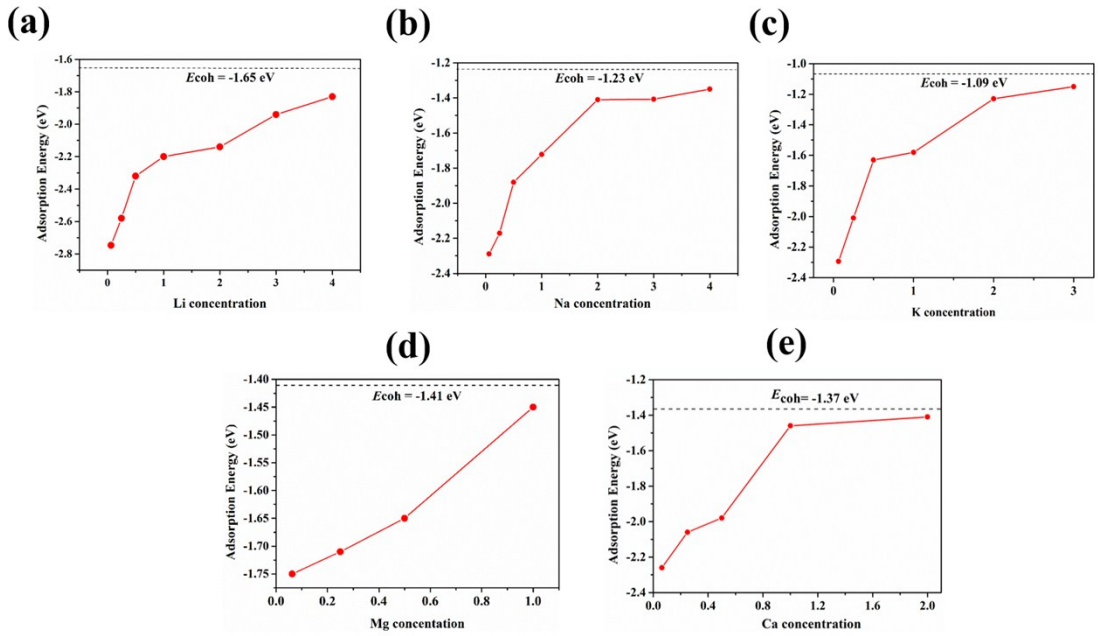

Fig. S15 The average adsorption energies per metal atom as a function of concentration x in the (a) Li_xFeSe, (b) Na_xFeSe, (c) K_xFeSe, (d) Mg_xFeSe and (e) Ca_xFeSe. The dashed lines denote the cohesive energies of the corresponding metal atoms in the bulk phases.

Note that the average adsorption energy (E'_{ave}) and cohesive energy in Fig. S15 are defined by the equations: $E'_{ave} = (E_{MxFeSe} - E_{FeSe} - xE_M)/x$, $E_{coh} = (E_{bulk} - n\ E_M)/n$, where E_{FeSe}, E_{MxFeSe}, and E_{bulk} are the total energies of monolayer FeSe, *M*-adsorbed FeSe, the bulk metal phase, and E_M is the energy of an isolated *M* atom, respectively, x is the number of adsorptions atoms, n is the number of *M* atoms in its bulk phase.

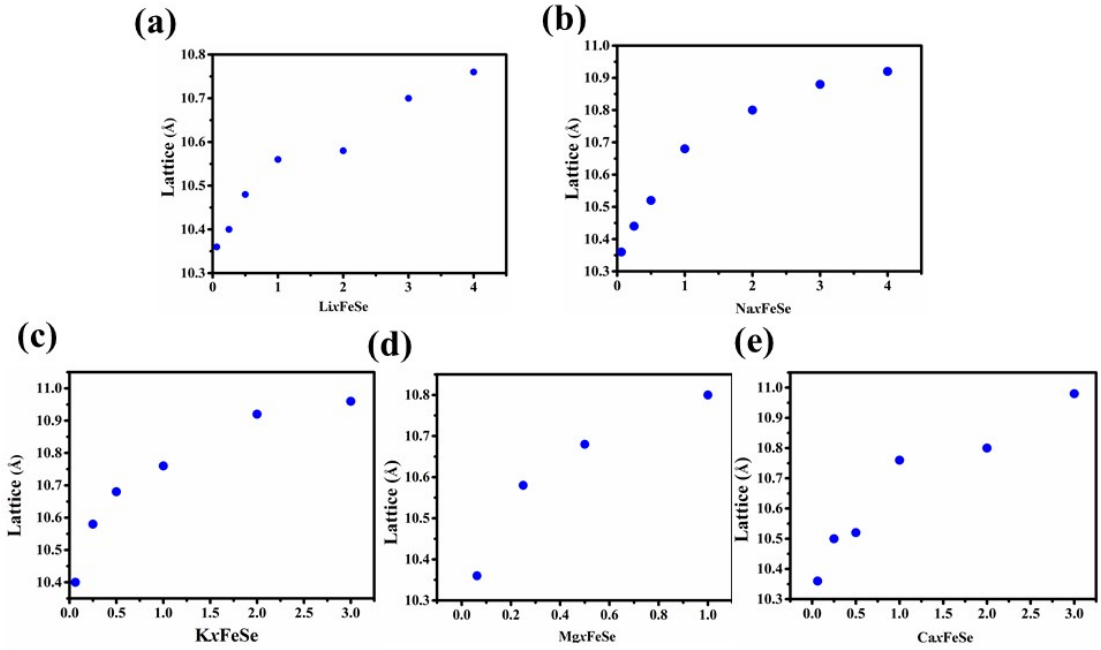

Fig. S16 The lattice constant variation as the function of *M* concentration *x*: (a) Li_xFeSe, (b) Na_xFeSe, (c) K_xFeSe, (d) Mg_xFeSe and (e) Ca_xFeSe.

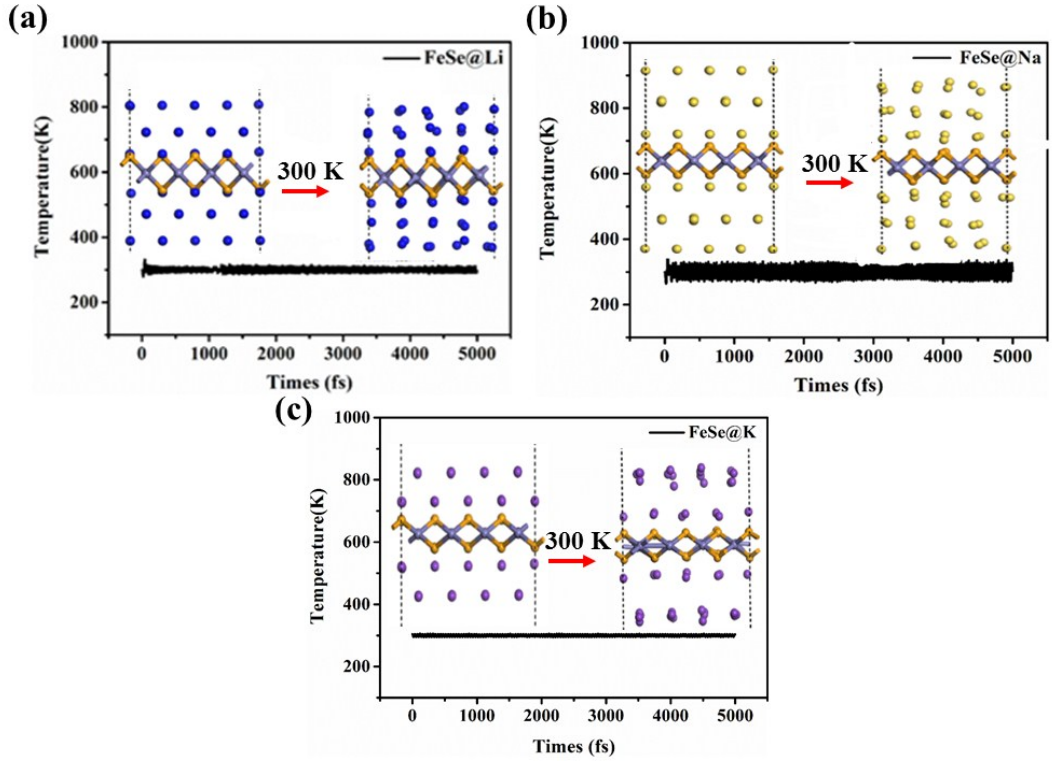

Fig. S17 The side views of the intercalated FeSe electrode by (a) Li, (b) Na , and (c) K atoms at the end of FPMD simulation, performed at 300 K.

Table S1. The calculated relative energies (in eV) of Li adsorbed at **A**, **B**, and **C** sites on the FeSe monolayer by BPE and PBE+U methods.

Methods	**A**	**B**	**C**
PBE	0.00	0.17	0.94
PBE+U	0.00	0.19	0.95

Table S2. In-plane stiffness (C_{11}, C_{22}, C_{12}, C_{66}, in N/m) and the Young's modulus (Y, in N/m) of the FeSe monolayers.

System	C_{11}	C_{22}	C_{12}	C_{66}	Y
FeSe	79.38	79.38	5.25	19.52	79.03
MoS_2	132.58	132.58	32.96	49.69	124.39

Table S3. The adsorption energy E_{ads} (in eV) of metal atom and the electron transfer (in e^-) from the adatoms to FeSe monolayer at the site **A**, **B**, and **C** at the PBE (PBE+U) level of theory. The largest E_{ads} are given in bold.

Metal	**E_{ads} (A)**	**E_{ads} (B)**	**E_{ads} (C)**	**Q (A)**	**Q (B)**	**Q(c)**
Li	**-2.75 (-3.60)**	-2.58 (-3.41)	-1.81 (-2.66)	0.93	0.91	0.88
Na	**-2.29 (-3.05)**	-2.16 (-2.95)	-1.58 (-2.34)	0.91	0.85	0.81
K	**-2.28 (-3.40)**	-2.18 (-3.28)	-1.83 (-2.97)	0.92	0.89	0.88
Mg	**-1.65 (-3.32)**	-0.51 (-2.47)	-0.29 (-1.65)	1.52	0.71	0.35
Ca	**-2.26 (-3.33)**	-0.73 (-1.80)	-0.22 (-0.85)	1.39	0.83	0.36

Table S4 The electron transfer (in e^-) from the metal atoms (M = Li, Na, K, Mg and Ca) to the FeSe monolayer and the Cl atom in their chlorides (LiCl, NaCl, KCl, $MgCl_2$ and $CaCl_2$).

	Li	Na	K	Mg	Ca
FeSe	0.93	0.91	0.92	1.52	1.39
Cl	0.92	0.86	0.88	1.61	1.56

Table S5. The average adsorption energy (E'_{ave}, in eV) for M multi-layer adsorption in the stoichiometry of M_xFeSe and the cohesive energy (E_{coh}, in eV) of M in bulk phase.

M_xFeSe	Li	Na	K	Mg	Ca
MFeSe	-2.20	-1.72	-1.58	-1.45	-1.46
M_2FeSe	-2.14	-1.43	-1.23	-1.40	-1.44
M_3FeSe	-1.94	-1.41	-1.15	-1.38	-1.41
M_4FeSe	-1.83	-1.35	-1.06	–	-1.35
E_{coh} (eV)	-1.65	-1.23	-1.09	-1.41	-1.37

Table S6. Changes in the lattice parameters and volume during the intercalation process of LIBs, NIBs, KIBs, MIBs, and CIBs.

System	Lattice (Å)	Expansion (Lattice)
FeSe	10.35	--
Li_4FeSe	10.76	3.90%
Na_4FeSe	10.92	5.50%
K_3FeSe	10.95	5.79%
MgFeSe	10.79	4.25%
Ca_3FeSe	10.97	5.99%